Available online at www.sciencedirect.com

ScienceDirect

Physics Procedia 76 (2015) 86 – 91

Physics Procedia

The 17th International Conference on Luminescence and Optical Spectroscopy of Condensed Matter (ICL2014)

The effect of Mg doping on structural and luminescent properties of Barium Strontium Titanate (BST)

A. Khare*, N. Chauhan

Department of Physics, National Institute of Technology, Raipur – 492 010 India

Abstract

Pure and Mg doped barium strontium titanate (BST) phosphor samples are prepared by solid state reaction (SSR) method at 1300°c. The prepared samples are characterized using X-ray diffraction (XRD), scanning electron microscopy (SEM) and UV-VIS absorption spectroscopy. The optical properties are studied in terms of mechanoluminescence (ML) and thermoluminescence (TL). The XRD results reveal perovskite structure of samples with XRD peaks corresponding to planes (100), (110), (111), (200) and (211). The SEM micrographs exhibit agglomeration of particles of different shapes. The particle size calculated using SEM and XRD data is found to lie in nano range. The ML intensity is found to depend on applied load while the TL intensity increases with increasing irradiation time.

Peer-review under responsibility of The Organizing Committee of the 17th International Conference on Luminescence and Optical Spectroscopy of Condensed Matter

*Keywords:*Solid state reaction; SEM; XRD; mechanoluminescence; thermoluminescence

1. Introduction

Luminescence of titanate based compounds has been extensively studied in crystalline samples during last decades. Various luminescent phenomena were observed in these semiconducting/insulating titanate based compounds. Barium strontium titanate ($Ba_{(1-x)}Sr_xTiO_3$; BST) is one of the most important perovskite ferroelectric

* Corresponding author. Tel.: +919425213445; fax: +917712254600.
*E-mail address:*akhare.phy@nitrr.ac.in

Peer-review under responsibility of The Organizing Committee of the 17th International Conference on Luminescence and Optical Spectroscopy of Condensed Matter
doi:10.1016/j.phpro.2015.10.016

materials, which is widely used for its solitary properties like, high dielectric constant, good stability, low dielectric constant loss, low current leakage, adjustable phase transition temperature etc. It offers various potential applications in the fields of electrically tunable microwave devices, DRAM, pyroelectric sensors, optoelectronics, in the development of environment friendly capacitors etc. [Praserthdam et al. (2014), Praserthdam et al. (2013)]. BST also is a good candidate for metal/rare earth doped host materials. There have been several reports of metal/rare earth doped BST thin films on structural and photoluminescence properties. The metal/rare earths can be doped in either A and/or B site of the perovskite material, which are relatively dependent on metal/rare earth's ionic radii [Zhang et al. (2012)]. In BST, Ba/Sr goes to A-site and Ti goes to B-site. The substitution of dopant on A-site requires the formation of negatively charged defects. The properties of BST strongly depend on the composition and characteristics of its constituent materials; so the variation in dopant concentration can lead to a better perovskite phosphor for which efforts are being made.

2. Experimental

To prepare nanocrystalline powder samples through solid state reaction (SSR) route, strontium carbonate ($SrCO_3$), barium cartbonate ($BaCO_3$), titanium dioxide (TiO_2) and magnesium dioxide (MgO_2) (all >99% pure) were taken as starting materials. First, stoichiometric amounts of raw materials were weighted and ball milled in acetone using Retsch PM 400 high energy ball mill operated at 200 rpm for 3 hours. After that obtained material was dried at room temperature for 12 hours. Further, the mixture was put into an alumina crucible and sintered at 1200^{o}C for 4 h in a digitally controlled electronic furnace in open air. After sufficient cooling, samples in the powder form were taken out of the furnace. Ball milling of starting materials helps in getting uniform and smaller size of particles. For different studies, nanocrystalline BST phosphors are prepared with different Ba: Sr ratio (x=0.1, x=0.2). The same was done for Mg doped BST powder. The specimen's morphologies and size of particles were examined using a ZEISS (model-EVO 18, German make) scanning electron microscope (SEM) while the powder XRD profiles of as-synthesized samples were recorded with X'pert powder PANalytical diffractometer using CuKα radiation (λ=0.1575nm) operated at 40kV voltage and 30mA anode current. The UV-Visible absorption spectra of the powder samples were recorded using a Shimadzu UV-VIS spectrophotometer (Model: UV-1700).

3. Results and Discussion

3.1 X-Ray Diffraction

The cubic phase of pure and Mg doped BST samples were confirmed by powder X-ray diffraction (XRD) patterns as presented in fig.1. The appearance of different peaks is same as reported earlier [Ioachim et al. (2007)]. These peaks in the pure samples are found corresponding to 2θ values of 22°, 31°, 39°, 45° and 56°. The assignment of peaks is done by comparison of observed peaks with standard JCPDS card no. 39-1395. The indexed planes are (100), (110), (111), (200) and (211). The clear observation of all BST diffraction peaks such as (100), (110) and (211) indicates that each sample shows ABO_3 cubic crystalline perovskite structures and the most intense (110) BST peaks in all specimens mainly grow along (110) orientations. The corresponding XRD data are summarized in table 1.

Table 1 XRD data of pure and Mg doped $Ba_{(1-x)}Sr_xTiO_3$ samples

Sample Name	2θ (degree)	FWHM (β) (radian)	Lattice spacing (d) (Å)	hkl	Crystallite size (D) (nm)
BST	22.24	0.0015	3.99	100	102.75
Pure	31.66	0.0022	2.82	110	73.37
	39.01	0.0022	2.31	111	72.30
	45.39	0.0033	1.99	200	51.11
	56.36	0.0021	1.63	211	82.08

BST	22.21	0.0013	4.00	100	123.46
Mg	31.62	0.0022	2.83	110	74.40
	38.96	0.0024	2.31	111	64.61
	45.29	0.0029	2.00	200	58.84
	56.28	0.0029	1.63	211	61.59

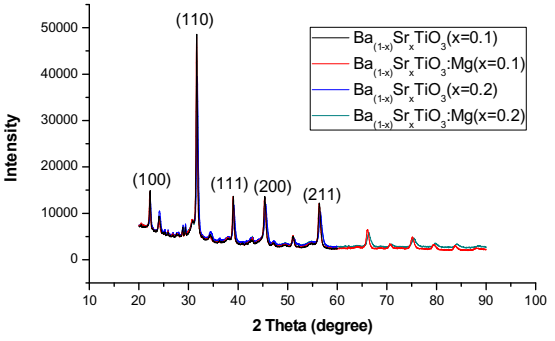

Fig. 1 X-ray diffractograms of pure and Mg doped $Ba_{(1-x)}Sr_xTiO_3$ (x=0.1, 0.2)

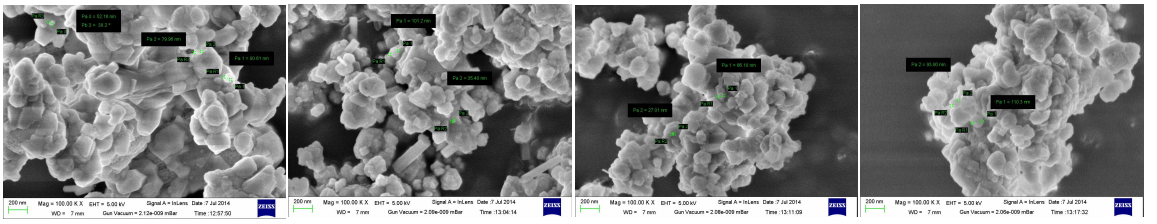

(a) (b) (c) (d)

Fig. 2 SEM images of **(a)** pure $Ba_{(1-x)}Sr_xTiO_3$ (x=0.1) **(b)** Mg doped $Ba_{(1-x)}Sr_xTiO_3$ (x=0.1) **(c)** pure $Ba_{(1-x)}Sr_xTiO_3$ (x=0.2) **(d)** Mg doped $Ba_{(1-x)}Sr_xTiO_3$ (x=0.2)

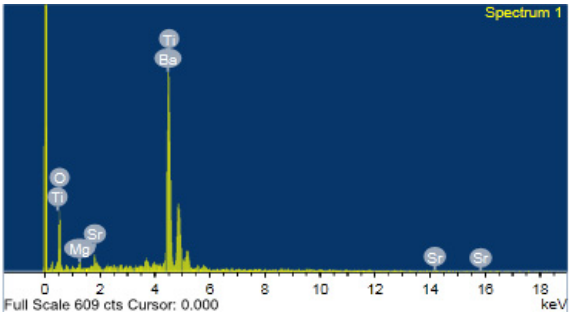

Fig. 3 EDX spectrum of BST: Mg

3.2 Scanning Electron Microscopy (SEM) and Energy Dispersive X-Ray (EDX) Spectrum

The SEM images of pure and Mg doped BST powder samples are presented in fig. 2 (a-d). All BST powder samples exhibit porous and uniform structure [Liu et al. (2004), Deshpande et al. (2005)]. In case of undoped BST samples, the SEM image fairly reveals uniform agglomerates with an average size of 90 nm. For the Mg doped samples the uniformity in distribution of particles improves and gets most uniform with highest Mg concentration. Another important finding is that average particle size increases with increasing dopant. From these images, it is inferred that in the samples with additives, better sintering and grain refining has taken place while in their absence the sample shows exaggerated grain growth. However, it is worth reporting that the grains in the pure BST samples possess hexagonal morphology, which upon addition of Mg shows increasing grain size and reduction in the volume ratio of the grain boundary region. The average grain sizes estimated from SEM images are in agreement with average grain size calculated from the XRD patterns, but in the samples the multimodal distribution of grains is not much reliable.

The EDX spectrum provides further information about the chemical compositions of the final products. The EDX profile of BST phosphor sample is shown in fig 3. These measurements confirm the presence of main constituents barium, strontium, titanium, oxygen and magnesium in the powder samples.

3.3 UV-Vis Absorption Spectroscopy

In order to find out band-gap values, absorption spectra of different BST phosphor samples in distilled water were recorded in the spectral region from 200 to 500 nm at room temperature (fig.4 (a)). The absorption profiles for all the samples exhibit sharp bands in the UV region. The fundamental absorption band for BST structure has been observed at about 210-235 nm. The relation between absorption coefficient (α) and the band-gap (E_g) is expressed as

$$\alpha = \frac{(h\nu - E_g)^{1/2}}{h\nu}$$

Where 'E_g' is the optical band-gap and 'ν' is the frequency of emitted light. Thus, as shown in fig. 3(b), the experimental band-gap values of different phosphor samples determined from the Tauc's plots are found to be 5.05, 5.50, 5.10 and 5.15eV. The lack of sharp structures in the spectrum presents difficulties in deriving an accurate E_g value, too.

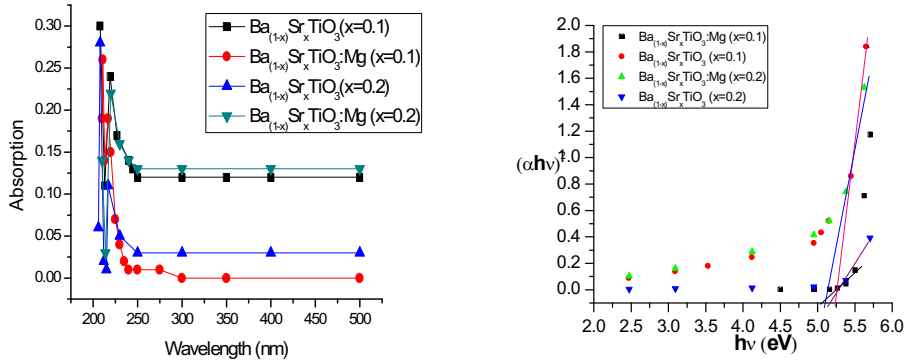

(a) (b)

Fig. 4 (a) Absorption spectra (b) Tauc's plot of pure and Mg doped $Ba_{(1-x)}Sr_xTiO_3$ (x=0.1, 0.2)

4. Luminescence studies

4.1 Mechanoluminescence

Fig. 5 shows the ML characteristics of BST sample induced by the impact of a moving piston onto the phosphors. The experiment was carried out for 400 gm load dropped from 55 cm height. A single peak is observed in ML intensity vs. time curve. The luminescence intensity depends upon load applied and impact velocity of the moving piston.

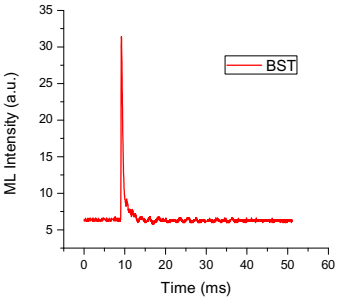

Fig.5 Variation in ML intensity of BST with time

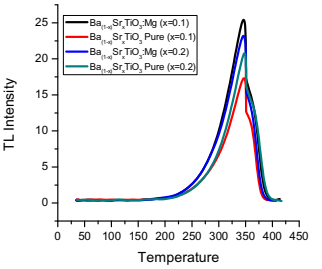

Fig.6 TL glow curve of pure and Mg doped $Ba_{(1-X)}Sr_xTiO_3$ (x=0.1, 0.2)

4.2 Thermoluminescence

The TL intensity of various BST samples was recorded upon irradiation of sample with UV light for 10 min. TL glow curves of these samples are presented in fig. 6. Glow curve is the term used to indicate the luminescence emitted from a thermo-luminescent phosphor immediately after irradiation. As observed from the figure, out of undoped samples (pure BST), the TL intensity is higher for the sample with greater Sr concentration while after addition of Mg, the TL intensity is found to be greater for the sample with lower concentration of Sr.

5. Conclusions

The XRD studies confirm the ABO_3 cubic perovskite structure of prepared samples while results of SEM studies exhibit uniform agglomeration of particles with an average size of 90 nm. By using Tauc's plots the band-gap values of different samples are estimated to be 5.05, 5.50, 5.10 and 5.15eV. The ML effect is instantaneous and ML intensity shows a sharp peak at the time of striking the sample. In the TL glow curve, the intensity is maximum for BST sample doped with 2 mol % of Mg impurity.

Acknowledgements

Authors are thankful to Chhattisgarh Council of Science and Technology (CCOST), Raipur, India for financial assistance under mini research project 2008/CCOST/MRP/2012 and Department of Metallurgical Engg. NIT Raipur, India for helping in taking XRD observations.

References

Ioachim A., Toacsan M.I., Banciu M.G., Nedelcu L., Vasiliu F., Alexandru H.V., Berbecaru C., Stoica G., 2007, Barium strontium titanate-based perovskite materials for microwave applications, Progress in Solid State Chemistry 35 513-520.

Khollam Y.B., Deshpande S.B., Potdar H.S., Bhoraskar S.V, Sainkar S.R., Date S.K., 2005, Simple oxalate precursor route for the preparation of barium strontium titanate: $Ba_{(1-x)}Sr_xTiO_3$ powders, Materials Characterization 54, 63–74.

Shen, C., Liu, Q., Liu, Qing-Feng, 2004, Photoluminescence properties of Er^{3+}-doped $Ba_{0.5}Sr_{0.5}TiO_3$ prepared by sol-gel synthesis, Material Science and Engineering B 111, 31-35.

Tubchareon, T., Soisuwan, S., Ratanathammaphan, S., Praserthdam, P., 2014, Effect of carbon-dopant on the optical band gap and photoluminescence properties of $[Ba_{0.5}Sr_{0.5}]TiO_3$ powders synthesized by the sol–gel process, Journal of Luminescence 145, 919–924.

Tubchareon, T., Soisuwan, S., Ratanathammaphan, S., Praserthdam, P., 2013, Effect of Na-, K-, Mg-, and Ga dopants in A/B-sites on the optical band gap and photoluminescence behaviour of [Ba0.5Sr0.5]TiO3 powders, Journal of Luminescence 142, 75–80.

Wang, J., Zhang, T., Pan, R., Ma, Z., Wang, J., 2012, Influence of Tm-doping on microstructure and luminescence behaviour of barium strontium titanate thick films, Applied Surface Science 258, 3283– 3288.